Preparation and Physical Properties of Wood/Polypropylene/Clay Nanocomposites

Hongkwan Lee, Dae Su Kim

Department of Chemical Engineering, Chungbuk National University, Cheongju, Chungbuk 361-763, Korea

Received 30 April 2008; accepted 8 September 2008
DOI 10.1002/app.29331
Published online 3 December 2008 in Wiley InterScience (www.interscience.wiley.com).

ABSTRACT: Wood plastic composites (WPCs) are attracting a lot of interests because they are economic, environmentally friendly, and show fairly good performance. To improve the performance of a wood/polypropylene (PP) composite, an organoclay was incorporated as a nanosize filler in this work. WPCs were prepared by melt blending followed by compression molding, and their performance was investigated by universal testing machine, izod impact tester, dynamic mechanical analyzer, thermal mechanical analyzer, differential scanning calorimetry, and TGA. Maleic anhydride polypropylene copolymer (MAPP) was used to increase compatibility between the PP matrix and wood particles and also improve the dispersion and exfoliation of the organoclay in the PP matrix. XRD analysis showed that the matrix of the WPCs with organoclay had intercalated structure. The SEM images of the WPCs with MAPP showed improved interfacial adhesion between the matrix and wood particles. The degree of water absorption increased with immersion time, but it could be restrained by incorporating MAPP. The performance of the WPCs was improved by the incorporation of the organoclay. © 2008 Wiley Periodicals, Inc. J Appl Polym Sci 111: 2769–2776, 2009

Key words: nanocomposites; polypropylene; wood particles; organoclay

INTRODUCTION

In recent years, thermoplastics reinforced with various natural fillers have received considerable attention because they have several advantages. Wood plastic composites (WPCs) have light weight, low cost, reasonable strength and stiffness, high filling levels, recycleability, biodegradability, renewable nature, and flexibility during the processing with no harm to the equipment. Moreover, WPCs can be readily processed by conventional plastic processing techniques such as extrusion, injection, and compression molding.[1,2] In addition, surface appearances can be controlled by adding different wood species and colored pigments.[3] The most common thermoplastics used in WPCs are high and low density polyethylene, poly(vinyl chloride), and polypropylene (PP).

When nonpolar PP or polyethylene (PE) was used as a matrix for WPCs, the incompatibility between the polymer and hydrophilic wood fillers has been a big problem, and there have been many studies on improving interfacial interactions between the polymer and wood fillers.[3–7] According to the previous studies, the best solution to the problem was using a coupling agent such as maleic anhydride functionalized polypropylene (MAPP). MAPP could bridge the interface and improve the stress transfer between the polymer matrix and wood fillers at low concentrations.[8]

Polymer/clay nanocomposites are a new class of polymeric materials that show improved properties at very low loading levels of a nanosize filler. The improved properties include mechanical, dimensional, thermal stability, and flame retardancy.[9–15] It has been suggested that the presence of clay in a polymer matrix can enhance the char formation, providing a transient protective barrier and hence, slowing down the degradation of the matrix.[9–10] Therefore, it was considered that a WPC with a polymer/clay nanocomposite matrix would improve the performance of the WPC. Some previous studies on WPCs with a polymer nanocomposite matrix have been reported.[16–18]

So, in this work, to improve the performance of a wood/PP composite, an organoclay was incorporated as a nanosize filler. PP has been one of the most common thermoplastics because it has low price and balanced properties.[19] It is difficult to get a good exfoliation and homogeneous dispersion of the silicate layers of clay in a nonpolar PP matrix even though an organoclay is used. However, it was encouraging that MAPP used generally as a coupling agent could assist the exfoliation and dispersion of organoclay in a PP matrix.[20,21] The effects of the organoclay on the performance of the WPCs were extensively studied by various test methods.

Correspondence to: D. S. Kim (dskim@chungbuk.ac.kr).

EXPERIMENTAL

Materials

PP (J-160, M_w = 219,300, density = 0.905 g/cm^3, melt flow index (MFI) = 16 g/10 min) was supplied by Honam Petrochemical Co., South Korea. Commercial PP functionalized with maleic anhydride (MAPP, Bondyram® 1004, M_w = 66,000, MFI = 90 g/10 min, MA contents = 0.8%, density = 0.90 g/cm^3) was obtained from Polyram Co., Israel. Wood flour (K0-008, poplar wood, particle size = 80 mesh) was supplied by Dongwon Chemical Co., South Korea. The wood flour was dried in a vacuum oven at 120°C for 24 h before use. The organoclay (Cloisite 20A, Southern Clay Products Co., Gonzales, TX) used was a natural montmorillonite modified with a dimethyl dehydrogenated tallow quaternary ammonium.

Preparation of WPCs

Wood flour/PP/organoclay nanocomposites were compounded in a Haake Rheomix 600 equipped with a roller blades rotor at 170°C, 60 rpm for 30 min. The fillers were loaded when the PP granules melted down enough to give a steady torque value. The WPC samples with the coupling agent of 0, 2, 3, and 5 wt % were denoted as W40P60, W40P58C2, W40P57C3, and W40P55C5 at a fixed wood content of 40 wt %, respectively, and the WPC sample with the organoclay 1 phr (part per hundred of PP resin) was denoted as W40P57C3M1. WPCs panels were prepared by compression molding in a Carver hydraulic hot press at 180°C, 1000 psi for 6 min. Specimens for thermomechanical testing were prepared by cutting the panels into desired sizes.

Mechanical tests

Tensile properties of the WPCs were measured using a universal testing machine (UTM, Lloyd LR-30K, Hampshire, UK) with a 1 kN load cell according to ASTM D882 at a crosshead speed of 5 mm/min. Izod impact tests were performed with unnotched WPC specimens at room temperature using an impact tester (SJI-103, Sungjin Co., South Korea) according to ASTM D256. For both tests, at least six specimens were tested for each WPC sample to obtain reliable test results.

Thermal characterization

TGA measurements for the WPCs were carried out using a thermal gravimetric analyzer (SDT 2960, TA instruments, New Castle, DE). Each TGA scan was performed under nitrogen purging from room temperature to 700°C at a heating rate of 10°C/min. Dynamic mechanical properties of the WPCs were measured using a dynamic mechanical analyzer (DMA 2980, TA instruments). WPC specimens were subjected to a sinusoidal displacement of 20 μm at a frequency of 1 Hz from 30 to 180°C at a heating rate 5°C/min. The melting behavior, glass transition temperature, and crystallinity of the WPCs were examined with a differential scanning calorimetry (DSC 2910, TA instruments) under nitrogen purging from −65 to 200°C at a heating rate of 5°C/min. The crystallinity (X_c) of each WPC sample was calculated using the following equation:

$$X_c = \frac{\Delta H_f 100}{\Delta H_f^0 w} \quad (1)$$

where, ΔH_f is the heat of fusion of the PP and various WPCs, ΔH_f^0 is the heat of fusion for 100% crystalline PP (ΔH_f^0 = 138 J/g)[22] and w is the weight fraction of the PP in the WPCs. Thermal expansion characteristics and dimensional stability of WPCs were investigated using a thermal mechanical analyzer (TMA 2940, TA instruments). TMA measurements were performed under nitrogen purging from room temperature to 160°C at a heating rate of 5°C/min.

Structure and morphology

XRD measurements were performed to investigate the structure of the WPCs using a Bruker D8 Discover X-ray diffractometer with Cu Kα radiation (λ = 1.5406 Å). The scanning rate and step size were 0.5°/min and 0.02° with 2θ varying from 0.6° to 40°. The d-spacing between the silicate layers of the clays were calculated using the Bragg's equation. The impact-fractured surfaces of the WPCs were observed using a scanning electron microscope (JSM-840A, JEOL Co., Japan) operated at an accelerating voltage of 20 kV. The specimens for the SEM were prepared by coating the surfaces with gold by sputtering.

Water absorption tests

A water bath with a temperature controller was used for immersion tests. The specimens were immersed in water at 40°C. The specimens were periodically taken out of the water, wiped with tissue paper to remove surface water, and then weighed. At least three specimens were weighed for each sample. Water absorption at any time t, $W_{a,t}$ was calculated using the following equation:

$$W_{a,t} = 100(W_{w,t} - W_d)/W_d \quad (2)$$

where, W_d and $W_{w,t}$ refer to the weight of the dry specimen and the wet specimen, respectively.

RESULTS AND DISSCUSION

Mixing process

The torque changes with mixing time for three WPC systems are shown in Figure 1. In all cases, an initial peak was observed as soon as the mixing process starts after loading a PP matrix system into the mixer. These initial peaks were due to the high viscosity of the PP matrix systems not melted yet. However, in about 4 min, all the PP matrix systems showed a low stable torque, indicating the completion of PP melting. The initial peak for W40P60 system was quite higher than the other two WPC systems because the WPC system did not comprise the MAPP.

The W40P60 and W40P57C3 composites were prepared by mixing for 15 min at 170°C. The MAPP of W40P57C3 composite was loaded together with PP at the beginning and the wood flour was added to the mixer after mixing the PP matrix system for 9 min. In preparing the W40P57C3M1 nanocomposite comprising the organoclay 1 phr, the PP matrix system with the MAPP and the organoclay was first mixed for 20 min after loading it to have enough time for a good exfoliation and dispersion of the organoclay in the PP matrix, and then additional 10-min mixing was followed after adding wood flour into the mixer. For the samples without organoclay, wood flour and PP was mixed for 6 min, whereas for the samples with organoclay, wood flour and PP was mixed for 10 min, because the torque value of both systems reached almost the same level. We focused on the torque decreasing with mixing time to determine the mixing time, and this is the reason why we conducted different durations of mixing for the two systems. The degree of abrupt torque rise observed just after adding wood flour was almost the same for three WPC systems because their wood flour contents were the same.

Mechanical properties

MAPP has been used as a coupling agent to enhance the compatibility between wood flour and PP. Sufficient MA groups attached onto the PP chains induce strong interfacial interaction due to the formation of chemical bonds between MA groups and hydroxyl groups of wood flours.[23] Incorporating just small amount of MAPP into a WPC system resulted in a drastic increase in tensile and impact strength at equal processing conditions.[24–26]

The mechanical properties of WPCs are listed in Table I. The effects of the coupling agent content and mixing temperatures on the mechanical properties of the WPCs were elucidated at a fixed wood flour content of 40 wt %.

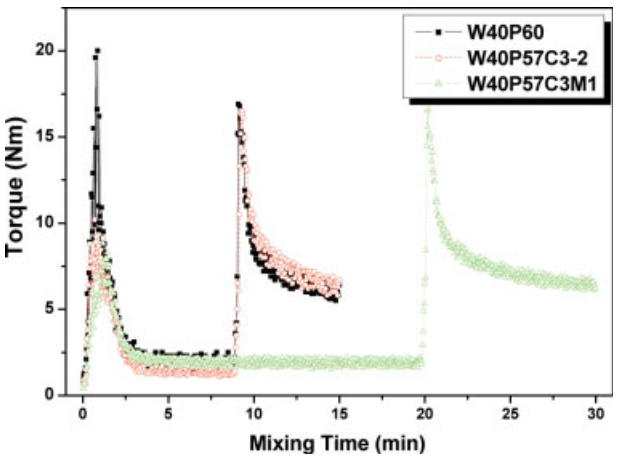

Figure 1 Torque change with mixing time. [Color figure can be viewed in the online issue, which is available at www.interscience.wiley.com].

Figure 2 shows the impact strength of W40P57C3 prepared at different mixing temperatures. The impact strength at 170°C was slightly higher than the other two. With increasing mixing temperature mixing effects would increase and result in an improvement in the mechanical properties of a WPC, but at the same time thermal degradation of the WPC would increase resulting in a decrease in the mechanical properties. Therefore, an optimum mixing temperature for the performance of the WPC should be determined first. From Figure 2, the mixing temperature of 170°C was considered an optimum mixing temperature for the WPC systems of this work. The WPC samples prepared at 175°C showed much darker in color because of thermal degradation compared with the other samples prepared at below 175°C.

As listed in Table I W40P55C5 showed almost the same mechanical properties as W40P57C3-2 even though it had more (5 wt %) coupling agent. Therefore, the coupling agent content of 3 wt % was considered an optimum value. The effects of incorporating the organoclay on the mechanical properties of the WPC system were also shown in Table I. The inclusion of the organoclay resulted in a slight improvement in the mechanical properties. Incorporated MAPP was also expected to improve the dispersion and exfoliation of the organoclay in the PP matrix. Zhang et al.[27] reported that the interlayer distance of silicates increased after the intercalation of MA groups and PP chains inside the clay layers.

Figure 3 shows the impact strength of the WPCs with different ingredients and compositions. Compared with W40P60, W40P57C3-2 comprising 3 wt % of MAPP showed a drastic increase in impact strength resulted from the coupling effects of MAPP at the interfaces. The impact strength of

TABLE I
Composition and Mechanical Properties of the WPCs

Sample types	Wood (wt %)	Polypropylene (wt %)	Coupling agent MAPP (wt %)	Montmorillonite Cloisite20A (phr)	Mixing time (min)	Mixing temperature (°C)	Tensile strength (MPa)	Tensile modulus (MPa)	Impact strength (kg_f-cm/cm^2)
W40P60	40	60	0	0	15	170	16.4 ± 0.4	1922.4 ± 422.0	5.6 ± 0.4
W40P58C2	40	58	2	0	15	170	31.0 ± 0.9	2270.8 ± 217.0	8.3 ± 1.7
W40P57C3-1	40	57	3	0	15	165	32.4 ± 1.0	2099.5 ± 336.3	8.5 ± 1.6
W40P57C3-2	40	57	3	0	15	170	33.2 ± 1.5	2295.5 ± 304.8	8.9 ± 1.3
W40P57C3-3	40	57	3	0	15	175	34.3 ± 1.4	2221.3 ± 74.8	8.8 ± 0.7
W40P55C5	40	55	5	0	15	170	35.8 ± 1.6	2211.6 ± 414.3	8.8 ± 1.6
W40P57C3M1	40	57	3	1	30	170	33.7 ± 1.1	2407.7 ± 305.6	9.0 ± 1.3

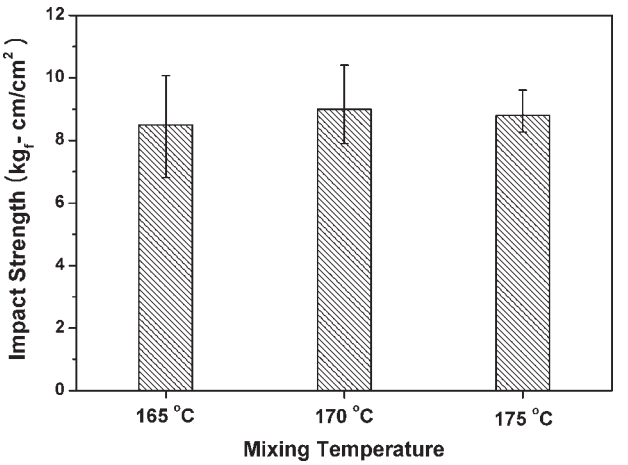

Figure 2 Impact strength of W40P57C3 prepared at different mixing temperatures.

W40P57C3M1 comprising 1 phr of the organoclay was slightly higher than that of W40P57C3-2, indicating a positive effect of the organoclay inclusion. W40P57C3M1 would have relatively higher absorption energy than the other WPCs without the organoclay during fracture processes because of the silicate layers of the organoclay in the PP matrix.

Thermal analysis

The thermal degradation behavior of the various WPCs was studied by TGA as shown in Figure 4. All the WPCs decomposed in two steps: wood particles first and then the PP matrix. The initial decomposition temperature at 5% weight loss of W40P57C3M1 increased from about 279°C to about 291°C compared with W40P57C3-2 due to the organoclay. The retard in the thermal degradation of W40P57C3M1 can be attributed to the decreased permeability of oxygen and the heat insulating

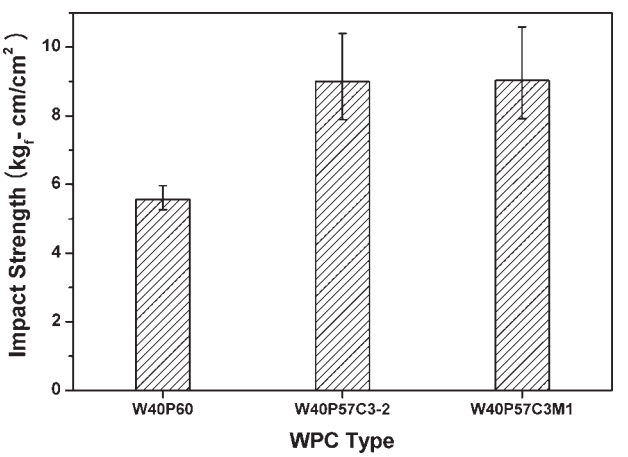

Figure 3 Impact strength of the WPCs.

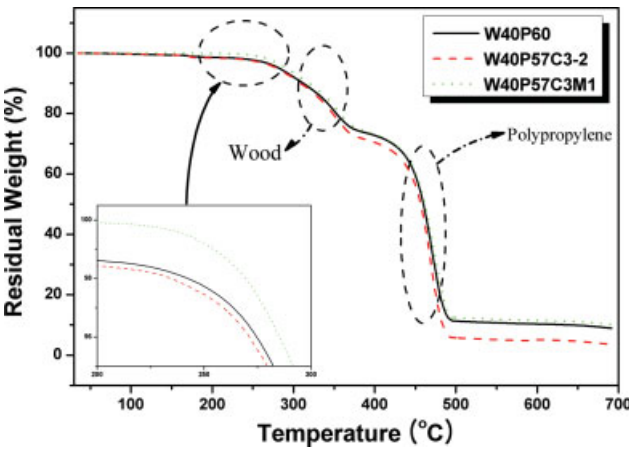

Figure 4 TGA curves for the WPCs. [Color figure can be viewed in the online issue, which is available at www.interscience.wiley.com].

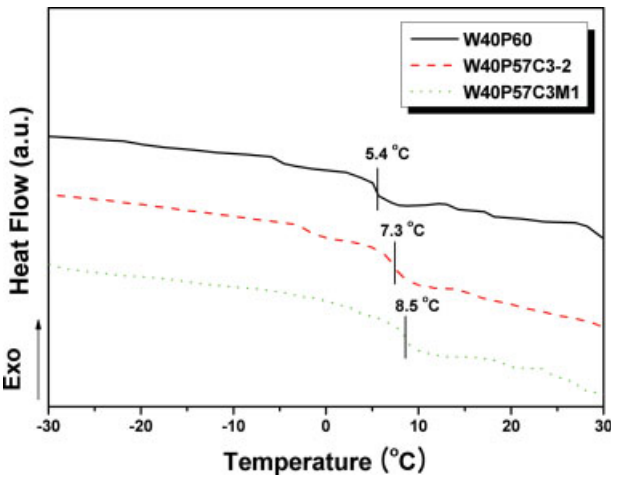

Figure 6 Glass transitions of the WPCs. [Color figure can be viewed in the online issue, which is available at www.interscience.wiley.com].

effects of the silicate layers in PP matrix. The reason why W40P60 showed a little bit retarded thermal degradation compared with W40P57C3-2 was considered due to the low thermal stability of the MAPP because W40P60 did not contain the MAPP.

The storage modulus of the WPCs is shown in Figure 5. The storage modulus of W40P57C3M1 was higher than those of the other WPCs. This increase in modulus could be attributed to a uniform distribution and a good interfacial adhesion between the organoclay and the polymer. Well dispersed clay particles with good interactions with a polymer matrix could improve the modulus considerably because they constrain the segmental motions of the polymer chains.[28]

The glass transitions of the WPCs are shown in Figure 6. The glass transition temperature of W40P57C3M1 was higher than those of the other WPCs. This increase in glass transition temperature could be attributed to a uniform distribution of the organoclay. Well dispersed clay particles with good interactions with a polymer matrix could improve the glass transition temperature because they constrain the segmental motions of the polymer chains.[28]

The crystallinity of W40P57C3-2 or W40P57C3M1 was higher than that of PP or W40P60 as shown in Table II, which lists T_m, ΔH_f, and X_c for various WPCs. The higher modulus of W40P57C3M1 could also be explained by the assumption that the silicate layers of the organoclay acted as efficient nucleating agents for the crystallization of the PP matrix.

The thermal expansion coefficients and dimension changes of various WPCs are listed in Table III. The dimensional stability of the W40P57C3M1 was higher than the other WPCs, because well-dispersed clay particles with good interactions with polymer matrix would also improve the interfacial adhesion considerably restricting thermally induced molecular motions.

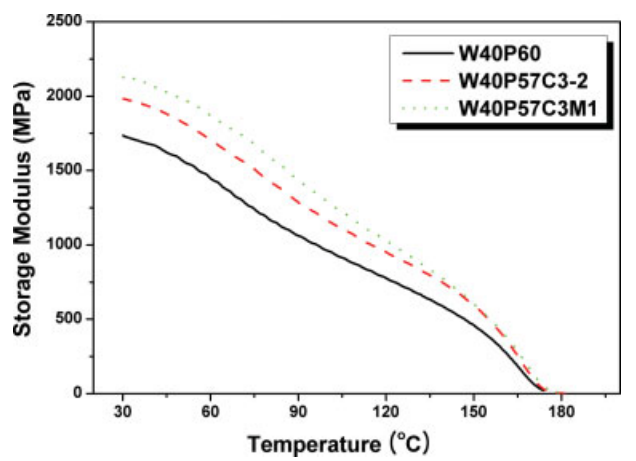

Figure 5 Storage modulus change with temperature for the WPCs. [Color figure can be viewed in the online issue, which is available at www.interscience.wiley.com].

Structure and morphology

The XRD curves of the organoclay (Cloisite 20A) and the WPC containing Cloisite 20A

TABLE II
T_m, ΔH_f, and X_c Data for Neat PP and the WPCs

Sample types	T_m (°C)	ΔH_f (J/g)	X_c (%)
PP	168.9	95.7	69.3
W40P60	165.1	57.7	69.7
W40P57C3-2	164.9	63.6	80.9
W40P57C3M1	165.3	65.5	83.3

TABLE III
The Thermal Expansion Coefficients and Dimension Changes of the WPCs

Sample types	α_1[a] [μm/m °C]	α_2[b] [μm/m °C]	ΔL[c] [%]
W40P60	103	194	0.69
W40P57C3-2	89	156	0.59
W40P57C3M1	74	153	0.54

[a] Expansion coefficient measured at 50°C.
[b] Expansion coefficient measured at 100°C.
[c] Dimension change between 50 and 100°C.

(W40P57C3M1) are shown in Figure 7. The XRD curves for the Cloisite 20A and W40P57C3M1 showed characteristic peaks at $2\theta = 2.6°$ and $2\theta = 1.7°$, respectively. The d_{001} peak of the organoclay shifted to lower angle. This shift suggested that the interlayer distance of silicates increased from 3.34 to 5.12 nm because of intercalation of polymer chains inside silicate layers of the organoclay.

The impact-fractured surfaces of WPCs specimens were observed by SEM as shown in Figure 8. Figure 8(a) shows the impact-fractured surface of W40P60 showing severe fiber pullout, debonding, and fibrillation. These observations for the WPC without MAPP were due to the poor adhesion between wood particles and the polymer matrix. Figure 8(b,c) are SEM images for W40P57C3-2 and W40P57C3M1, respectively. Both SEM images showed almost the same morphology because the presence of MAPP resulted in a good interfacial adhesion between the polymer matrix and wood particles.

Water absorption

The water absorption behavior of the WPCs in a hydrothermal environment was shown in Figure 9.

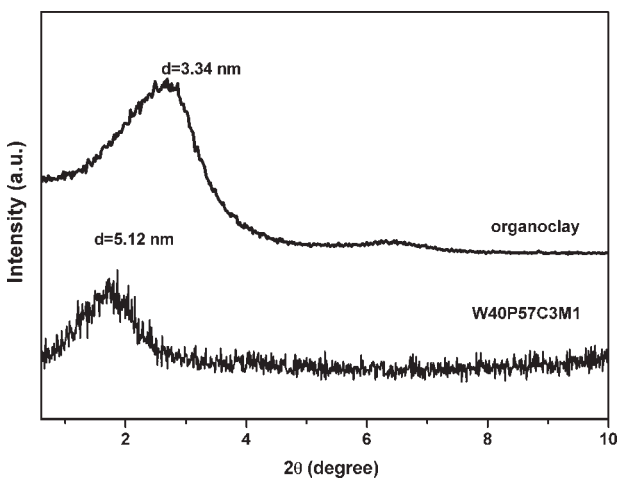

Figure 7 XRD patterns of the organoclay and W40P57C3M1.

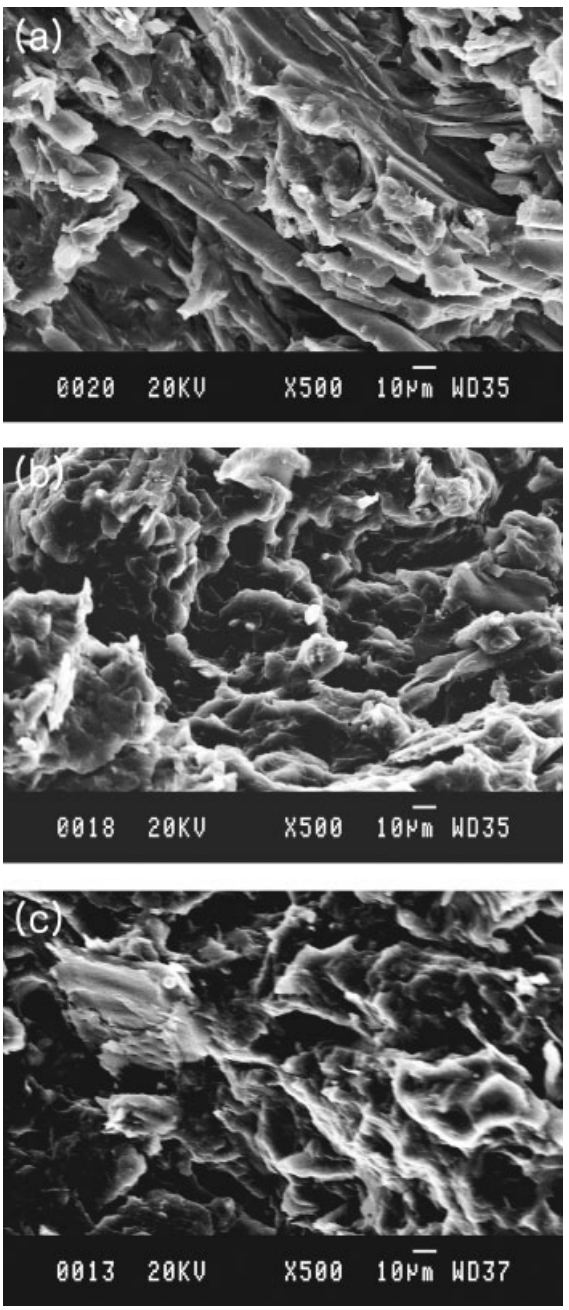

Figure 8 SEM images of the impact-fractured surfaces of (a) W40P60, (b) W40P57C3-2, and (c) W40P57C3M1.

As expected, the degree of water absorption increased with increasing immersion time. The degree of water absorption of W40P60 was considerably higher than the other two WPCs because W40P60 had weak interfacial adhesion between wood particles and the polymer matrix as shown in Figure 8(a). Weak interfacial adhesion would make a lot of channels for water absorption at the interfaces. On the other hand, the degree of water absorption of W40P57C3M1 was slightly lower than W40P57C3-2. From this result, it was considered that

W40P57C3M1 had a little bit stronger interfacial adhesion and hydrophobicity than W40P57C3-2 due to the organoclay.

Figure 10 shows the tensile strength of various WPCs as a function of immersion time. The tensile strength of all the WPCs decreased with immersion time and then eventually leveled off. The penetration of a large amount of water into the WPCs would lead to a decrease in the interfacial adhesion between wood particles and the polymer matrix. W40P57C3-2 and W40P57C3M1 showed almost the same trend in the tensile strength decrease with immersion time because they showed almost the same water absorption behavior as shown in Figure 9. The tensile strength of W40P60 leveled off after 24 h even though water absorption increased continually with immersion time as shown in Figure 10. This result was considered due to weak interfacial adhesion of W40P60 because only the PP matrix would resist to the tensile deformation with negligible reinforcing effects of wood fibers, and the increase in water absorption mainly occurred to fill the channels at the interfaces and wood fibers does not affect too much the tensile resistance of the hydrophobic polymer matrix. However, the tensile strength of W40P57C3-2 and W40P57C3M1 decreased with immersion time up to 168 h because the strong interfacial adhesion that helped load transfer at the polymer-wood fiber interfaces would be gradually deteriorated with the increase of water absorption. It was noticeable that the ultimate tensile strength of W40P57C3-2 and W40P57C3M1 at a long immersion time was considerably higher than that of W40P60 because of the strong interfacial adhesion.

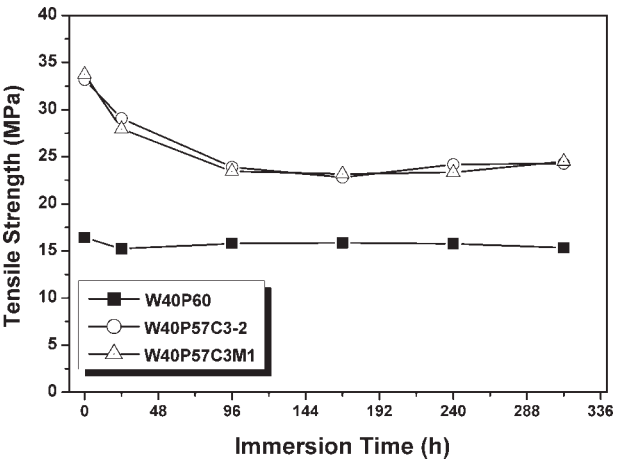

Figure 10 Tensile strength with immersion time.

CONCLUSIONS

Wood/PP/clay nanocomposites were well prepared by melt blending. According to XRD analysis, the PP matrix of the WPCs with organoclay showed intercalated structure. The inclusion of the organoclay by 1 phr improved the tensile properties, impact strength, thermal stability, glass transition temperature, and crystallinity of the WPC system slightly though the storage modulus increased considerably. The dimensional stability and antiwater absorption property of the WPC system were improved slightly by the inclusion of the organoclay. The SEM images of the WPCs with MAPP showed considerably improved interfacial adhesion between the matrix and wood particles. The degree of water absorption increased with immersion time, but it could be restrained by incorporating MAPP that increased the interfacial adhesion. The performance of the WPCs was improved by the incorporation of the organoclay.

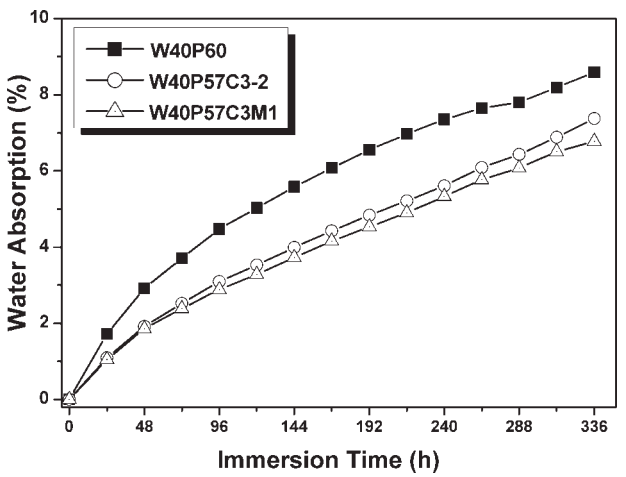

Figure 9 Water absorption with immersion time.

References

1. Ismail, H.; Salmah, A.; Nasir, M. Polym Test 2001, 20, 819.
2. Oksman, K.; Clemons, C. J Appl Polym Sci 1998, 67, 1503.
3. Bledzki, A. K.; Reihmane, S.; Gassan, J. Polym Plast Technol Eng 1998, 37, 451.
4. Stain, M. M.; Kokta, B. V.; Imbert, C. Polym Plast Technol Eng 1994, 33, 89.
5. Felix, J. M.; Gatenholm, P. J. J Appl Polym Sci 1993, 50, 699.
6. Maldas, D.; Kokta, B. V. Compos Interfaces 1993, 1, 87.
7. Gauthier, R.; Joly, C.; Coupas, A.; Gauthier, H.; Escoubes, M. Polym Compos 1998, 19, 287.
8. Krzysik, A. M.; Youngquist, J. A.; Myers, G. E.; Chahyadi, I. S.; Kolosick, P. C. In Wood Adhesives 1990: Proceedings of a Symposium. Conner, A. H.; Christiansen, A. W.; Myers, G. E.; Eds. Forest Products Research Society; Madison, WI, 1991; p 183.
9. Zanetti, M.; Lomakin, S.; Camino, G. Macromol Mater Eng 2000, 279, 1.
10. Zhang, S.; Horrocks, A. R. Prog Polym Sci 2003, 28, 1517.
11. Bourbigot, S.; Gilman, J. W.; Wilkie, C. A. Polym Degrad Stabil 2004, 84, 483.
12. Gong, F.; Feng, M.; Zhao, C.; Zhang, S.; Yang, M. Polym Degrad Stabil 2004, 84, 289.
13. Qin, H.; Su, Q.; Zhang, S.; Zhao, B.; Yang, M. Polymer 2003, 44, 7533.

14. Marosi, G.; Márton, A.; Szép, A.; Csontos, I.; Keszei, S.; Zimonyi, E. Polym Degrad Stabil 2003, 82, 379.
15. Beyer, G. Plast Additives Compound 2002, 10, 22.
16. Liao, H.-T.; Wu, C.-S. Macromol Mater Eng 2005, 290, 695.
17. Guo, G.; Park, C. B.; Lee, Y. H.; Kim, Y. S.; Sain, M. Polym Eng Sci 2007, 47, 330.
18. Guo, G.; Wang, K. H.; Park, C. B.; Kim, Y. S.; Li, G. J Appl Polym Sci 2007, 104, 1058.
19. Ahmed, M. Textile Science and Technology; Elsevier: Amsterdam, 1982.
20. Jeon, H. G.; Jung, H. T.; Lee, S. D.; Hudson, S. Polym Bull 1998, 41, 107.
21. Manias, E.; Touny, A.; Wu, L.; Lu, B.; Strawhecker, K.; Gilman, J. W.; Chung, T. C. Polym Mater Sci Eng 2000, 82, 282.
22. Joseph, P. V.; Joseph, K.; Thomas, S.; Pillaic, C. K. S.; Prasad, V. S.; Groeninckx, G.; Sarkissova, M. Compos Appl Sci Manuf 2003, 34, 253.
23. Kim, H. S.; Lee, B. H.; Choi, S. W.; Kim, S.; Kim, H. J. Compos Appl Sci Manuf 2007, 38, 1473.
24. Bledzki, A. K.; Farnk, O.; Huque, M. Polym Plast Technol Eng 2002, 41, 435.
25. Li, T. Q.; Li, R. K. Y. Polym Plast Technol Eng 2001, 40, 1.
26. LeThi, T. T.; Gauthier, H.; Gauthier, R.; Chobert, B.; Guillet, J.; Luong, B. V.; Nguyen, V. T. J Macromol Sci Pure Appl Chem 1996, 331997.
27. Zhang, Y. Q.; Lee, J. H.; Rhee, J. M.; Rhee, K. Y. Compos Sci Technol 2004, 64, 1383.
28. Ajayan, P. M.; Schadler, L. S.; Braun, P. V. Nanocomposites Science and Technology; Wiley-VCH: Weinheim, 2003.